Dynamic response of a double barrier system: The effect of contacts

T. C. Au Yeung,[1] Yabin Yu,[2] W. Z. Shangguan,[1] and W. K. Chow[2]
[1]*School of Electrical and Electronic Engineering, Nanyang Technological University, Singapore 639798*
[2]*The Hong Kong Polytechnic University, Department of Building Services Engeering, Hong Kong, People's Republic of China*
(Received 2 December 2002; published 25 August 2003)

We study the dynamical response of a double-barrier conductor with two contacts to investigate the contact effect on ac conduction in the system. We have presented the calculation of various physical quantities such as the distributions of internal potential and charge density, capacitance and low-frequency ac conductance. We show that the characteristic potentials would tend to unity (zero) in the reservoirs. When the system is far away from resonance, the charge distribution exists only around the barrier regions as a response to the applied voltage, and hence the contacts almost have no effect on the results. In the case of small transmission probability, we find a considerable amount of charge distribution surrounding the double-barrier conductor. As for the resonant case or near the resonance, our results show that the charge distribution displays large fluctuations outside the conductor, but almost no charge distribution within the conductor. In this case, the effect of contacts on the charge and potential distributions is considerable. Moreover, we find that qualitatively the presence of contacts does not change the main features of the emittance without contacts. But the contact effect on the capacitance is significant when the chemical potential is very close to resonant energy: there is a sharp capacitance peak at resonance that does not exist in the case without contacts.

DOI: 10.1103/PhysRevB.68.075316 PACS number(s): 73.21.−b, 73.63.−b, 72.10.−d

I. INTRODUCTION

The transport properties of mesoscopic conductor systems have been studied extensively, both theoretically and experimentally. One of these studied systems is the one-dimensional device connected to wide reservoirs involving the electron-electron (e-e) interaction which is of fundamental importance.[1,2] The contacts play an important role in the conductance[3–7] due to its significant interaction with conductors.[8] The effect of e-e interaction on quantum transport in quantum wire (QW) was investigated using the Luttinger-Liquid model, which explains the renormalization of charge-wave density and gives the standard dc conductance steps e^2/h.[1,3–5,9] For the ac case, the ac response is strongly sensitive to the distribution of potential inside the sample.[10–14] Büttiker *et al.* have discussed extensively the current conservation and gauge invariance for ac transport in the presence of e-e interaction.[14–17] They formulated the theory of ac conductance in the regime of linear response and low frequency based on both continuous and discrete internal potential models. There were further works on the ac transport in QW with contacts. Blanter *et al.* adopted the random-phase approximation to calculate the ac admittance in the presence of e-e interaction.[18] Sablikov *et al.* used the Hartree-Fock approximation for electron wave functions to investigate the internal potential and electron-density distributions in QW.[8] Also, Sablikov and Shchamkhalova studied the one-dimensional e-e interaction using the Bosonization technique.[19] They obtained different ac (low frequencies) transport properties such as electron-density distribution and quantum wire impedance compared to that of the Luttinger-Liquid model with short-range interaction.

On the other hand, the double-barrier-resonant-tunneling nanostructures (DBRTNS) also have attracted great research interest because of their many potential device applications, and their significance in the study of the physics of confined structures. Büttiker *et al.* applied their theory of ac transport (in the regime of linear response and low frequency) to DBRTNS based on the discrete potential model.[15] A detailed analysis for a larger range of frequencies and for a nonlinear case associated with mesoscopic conductors can also be done by Büttiker and Christen.[20] Moreover, Zhao *et al.*[21] used the continues potential model to study the internal potential and charge-density distributions in DBRTNS. Shangguan *et al.* followed up to investigate in detail the ac emittance and the electrochemical potential, taking into account also the temperature effect.[22] They found that for very low temperature, the charge accumulation is very small in the resonant cases and in the cases of zero transmission probability; and for cases in which the transmission probability is large but less than one (near resonance), the charge accumulation is large.

However, so far the effect of contacts (reservoirs) on ac transport in DBRTNS has not yet been investigated quantitatively. In this paper, we consider the DBRTNS with contacts as a whole system and study how the wide contacts affect the ac transport properties such as internal potential, charge accumulation, ac emittance, and so on. The left and right contacts we consider are identical and two dimensional (2D), and the DBRTNS is one dimensional. We use the hyperbolic tangent function to represent the 2D contacts in such a way that the transverse dimension of the contacts varies slowly with distance. Thus, the transverse energy levels are slowly varying functions of distance in the transition region from the contacts to the double barrier. In this case, we assume, as a good approximation, that there is no coupling between all the transverse channels in the scattering process of charge carriers. Hence, each charge carrier will be all the way in a single channel throughout the scattering process without being scattered into the other channels. This approximation much simplifies the calculation of scattering wave

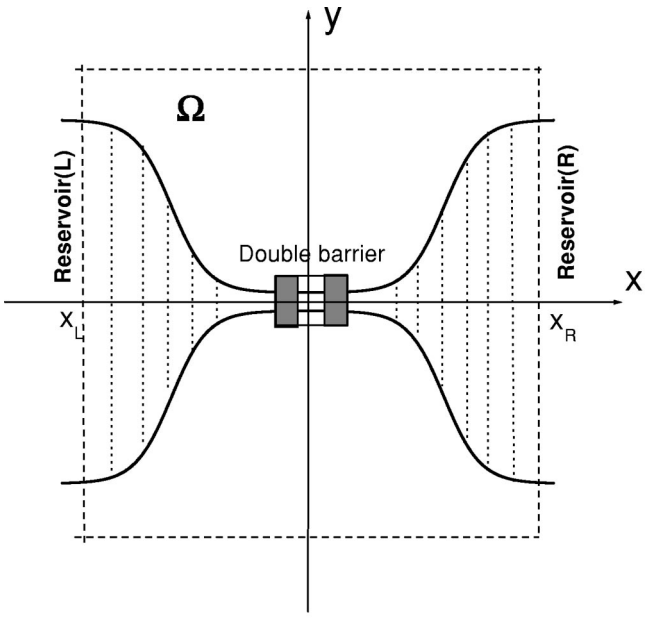

FIG. 1. Schematic view of a double-barrier structure with two reservoirs. The Ω is a imagined volume, and it is assumed that no electric-field line penetrates the surface of Ω.

functions and scattering matrix. The internal potential, governed by a 3D Poisson equation, is assumed to be 1D. That means, it is only a function of the distance in the longitudinal direction. So we can integrate the Poisson equation over the transverse direction and the equation will involve the variable cross-sectional area (due to the different cross-sectional areas of the contacts and wire).

II. MODEL AND THEORY

The model of the double barrier with reservoirs that we consider in this paper is a two-dimensional–one-dimensional–two-dimensional system (see Fig. 1). In the center of this system is a conductor of double-barrier structure. We assume that the width of the system as a function of x is

$$w(x)=a+\frac{W-a}{2}\left[\tanh\left(-\frac{2(x+L_{c0})}{L_c}\right)+1\right] \quad \text{for } x<0,$$

$$w(x)=a+\frac{W-a}{2}\left[\tanh\left(\frac{2(x-L_{c0})}{L_c}\right)+1\right] \quad \text{for } x>0.$$

Here, a and W are the widths of 1D portion and reservoirs (2D), respectively. L_c describes the size of the transition regions between the reservoirs and 1D portion, and $2L_{co}$ is equal to the distance between the centers of the left and right transition regions. Furthermore, we use b for the barrier width and $2c$ for the well width. We will investigate the linear response of the system to a time-dependent external voltage. When the voltage is applied to the two reservoirs, besides the process in which electrons are injected into the 1D transverse channels and then undergo scattering by the contacts and double barrier, we have to consider the pile-up charge and the induced internal electrostatic potential in the system, which affect the transport of the electrons in the systems. To proceed, we imagine a volume Ω (the dashed-line box in Fig. 1), which encloses the entire conductor and parts of the reservoirs and is large enough to include all the varying distributions of the potential and charges. This means that all the electric-field lines come from and end at the charges inside Ω.

In order to calculate the dynamics response of the double-barrier system, according to Büttiker's theory, we have to calculate the injectivity $dn_\alpha(\mathbf{r})/dE$ and the local density of states (LDOS) $dn(\mathbf{r})/dE=\Sigma_\alpha dn_\alpha(\mathbf{r})/dE$ (Refs. 10,14,15) for the system (here $\alpha=1$ or L for the left contact and $\alpha=2$ or R for the right contact. Because our interest is electron transport in the longitudinal direction (the x direction, say). We will assume that the potential and charge-density distributions are one dimensional. Accordingly, we will only calculate the injectivity $dn_\alpha(x)/dE=\int dn_\alpha(\mathbf{r})/dEdy$ and the density of states $dn(x)/dE=\int dn(\mathbf{r})/dEdy$. To do this, we first calculate the electron wave function of the incoming scattering state (from the left). In the reservoirs, the wave functions read

$$\Psi_l^L(x,y)=(e^{ik_l^x x}+s_{11,l}e^{-ik_l^x x})\phi_l^W(y) \quad \text{for } x\ll -L_{co}-L_c, \tag{1}$$

$$\Psi_l^R(x,y)=s_{21,l}e^{ik_l^x x}\phi_l^W(y) \quad \text{for } x\gg L_{co}+L_c, \tag{2}$$

where $\phi_l^W(y)$ are the transverse eigenfunctions of the reservoirs, $k_l^x=[2m^*E/\hbar-(l\pi/W)^2]^{1/2}$ are the wave numbers defined in the x direction, m^* is the effective mass of electrons, and E is the energy of the electron. In the transition regions between 1D and 2D portions, we plot vertical lines to divide the regions into a series of narrow layers (see Fig. 1). In the narrow layers labeled by $i=1,2,3,\ldots$, the wave functions can be expressed as

$$\Psi_l^{(i)}(x,y)=\sum_{l'}[A_{l'l}e^{ik_{l'}^{(i)}x}+B_{l'l}e^{-ik_{l'}^{(i)}x}]\phi_{l'}^{(i)}(y), \tag{3}$$

where $\phi_{l'}^{(i)}(y)$ are the transverse eigenfunctions in layer i, $k_l^{(i)}=[2m^*E/\hbar-(l\pi/W_i)^2]^{1/2}$, and W_i is the width of the layer i. In this paper, it is assumed that the width variation in the transition regions is so slow that we can ignore the state hopping as the wave functions propagate through the layers, and then Eq. (3) simplifies as

$$\Psi_l^{(i)}(x,y)=(A_l^{(i)}e^{ik_l^{(i)}x}+B_l^{(i)}e^{-ik_l^{(i)}x})\phi_l^{(i)}(y). \tag{4}$$

In the 1D portion (i.e., the double barrier together with the left and right leads), the wave functions may be expressed as

$$\Psi_l^I(x,y)=(A_l^{(I)}e^{ik_l^{(I)}x}+B_l^{(I)}e^{-ik_l^{(I)}x})\phi_l^{1D}(y), \tag{5}$$

where $I=1,\ldots,5$ represent the regions of two barriers, well, and the two 1D leads, respectively. $\phi_m^{1D}(y)$ are the transverse eigenfunctions of electrons in the 1D portion, $k_l^x=[2m^*(E-U_I)/\hbar-(l\pi/a)^2]^{1/2}$, and U_I is the double-barrier potential:

$$U_I = \begin{cases} U_0 & \text{in the barriers,} \\ 0 & \text{otherwise.} \end{cases}$$

Using continuity of Ψ_l and $\partial\Psi_l/\partial x$ at the boundaries between neighboring layers, we determine the wave functions of the electrons in the system, and then the injectivity[11]

$$\frac{dn_L(x)}{dE} = \sum_l \int dE \left(\frac{-\partial f}{\partial E}\right) \int dy \frac{1}{hv_l} |\psi_l(x,y)|^2, \quad (6)$$

where $v_l = \hbar k_l^x / m^*$ is the incident velocity of the electrons in the direction of transport (x axis). Furthermore, for our symmetrical system,

$$\frac{dn_R(x)}{dE} = \frac{dn_L(-x)}{dE}, \quad (7)$$

and the LDOS is then given by

$$\frac{dn(x)}{dE} = \frac{dn_L(x)}{dE} + \frac{dn_R(x)}{dE}. \quad (8)$$

Meanwhile, the scattering matrices s_{11} and s_{21} are given by Eqs. (1) and (2). In the presence of a small and low-frequency ac voltage v_{ac} applied to the reservoir α ($\alpha = 1$ or L for the left reservoir and $\alpha = 2$ or R for the right reservoir), the internal potential $U(x)$ is given by $U(x) = u_\alpha(x) v_{ac}$, where u_α is the characteristic function. Using the Thomas-Fermi approximation, the characteristic function u_α satisfies the Poisson equation:[14,15]

$$-\nabla^2 u_\alpha + \frac{e^2}{\varepsilon_0} \frac{dn(\mathbf{r})}{dE} u_\alpha(x) = \frac{e^2}{\varepsilon_0} \frac{dn_\alpha(\mathbf{r})}{dE}, \quad \alpha = 1,2. \quad (9)$$

Under the Thomas-Fermi approximation, the second term in Eq. (9) gives the induced charges in the conductor and the third term gives clearly the injected charges. As has been pointed out by Büttiker and Christen,[24] The Thomas-Fermi approximation is not well justified and permits us to obtain an estimate only. In this paper, we do not attempt to make a very accurate calculation, and our interest is to present a qualitative estimate for the potential and charge distributions. In Eq. (9) we have neglected the variation of the potential with y and z, and assume that the characteristic function is a function of x only. This assumption is reasonable, because the variation of potential, in fact, is induced by electrochemical potential difference $\delta\mu$ (or external voltage δV) between the left and the right sides. We obtain the following equation by integrating over y and z and using $\int dy dz |\phi(z,y)|^2 = 1$ (for convenience of presentation, we only mentioned about the coordinate y in the above discussion):

$$-\frac{d^2 u_\alpha(x)}{dx^2} + \frac{e^2}{\varepsilon_0 A(x)} \frac{dn(x)}{dE} u_\alpha(x) = \frac{e^2}{\varepsilon_0 A(x)} \frac{dn_\alpha(x)}{dE}, \quad (10)$$

where $A(x) = d \times w(x)$ is the cross-sectional area of the double-barrier structure, d is the thickness of the system.

III. INTERNAL POTENTIAL AND CHARGE DENSITY

We first calculate the internal potential $u_\alpha(x)$ by numerically solving the Poisson equation (10), and then obtain the induced charge distribution. To solve Eq. (10) for $u_\alpha(x)$, we need the boundary values of $u_\alpha(x)$. Here we use the neutrality condition[14] to determine the boundary values of $u_\alpha(x)$:

$$u_\alpha(x_L) = \frac{dn_\alpha(x_L)}{dE} \Big/ \frac{dn(x_L)}{dE},$$

$$u_\alpha(x_R) = \frac{dn_\alpha(x_R)}{dE} \Big/ \frac{dn(x_R)}{dE}, \quad (11)$$

where x_L and x_R are left and right boundary lines of the region Ω (see Fig. 1), which is a volume[14–16] that is so large that electric-field lines through the surface of it vanish, i.e., the electric field is completely screened within the volume. If the reservoirs are very large (the width W is very large), then from Eq. (11) we conclude that the boundary values $u_1(x_L) \times [u_2(x_R)]$ and $u_1(x_R)[u_2(x_L)]$ are very close to unity and zero, respectively. In our case, the boundary values are close to unity or zero. When our system is biased by a small voltage δV (applied to reservoir α), the distribution of charge density in Ω is given by $\delta q(x) = \rho(x)\delta V$, where

$$\rho(x) = \frac{dq(x)}{dV} = -\varepsilon_0 A(x) \frac{d^2 u_\alpha(x)}{dx^2}$$

$$= e^2 \left[\frac{dn_\alpha(x)}{dE} - \frac{dn(x)}{dE} u_\alpha(x) \right]. \quad (12)$$

In Fig. 2, we present the distribution of internal potential $u = u_1(x)$ and charge density $\rho(x)$ for various Fermi levels $\mu (= \mu_L = \mu_R)$ at temperature $T = 0$. As is aforementioned, we use $\Delta = h^2/8m^*a^2$, the energy of the transverse ground state in the 1D leads as a unit of energy, and the width a of the leads as a unit of distance. In our calculation, we set $a = 50$ nm, $d = a/2$ (the thickness of our system), and $x_L = -x_R$.

Figure 2(a) shows the results for $\mu = 1.805$, which corresponds to the resonant case where the Fermi level equals the resonant energy of the double-barrier structure, and for an open channel the transmission probability equals unity. In this case, one finds that the potential drops mainly appear in the transition regions between the 1D and 2D portions, and basically there is no potential drop across the double barrier although we find some oscillations in the potential in the 1D leads. Furthermore, for the resonant case, the charge density shows intensive fluctuations around zero beyond the double barrier, while inside the double barrier there is almost no charge accumulation. This reflects the effect of contacts on the distributions of potential and charge density. We know that the injected electron density is proportional to the square of the amplitude of the electron wave function which is oscillating along the x direction. Thus, the distribution of the injected electron density consists of alternative layers of more negative charges and less negative charges. This would be the total charge-density distribution should there be no

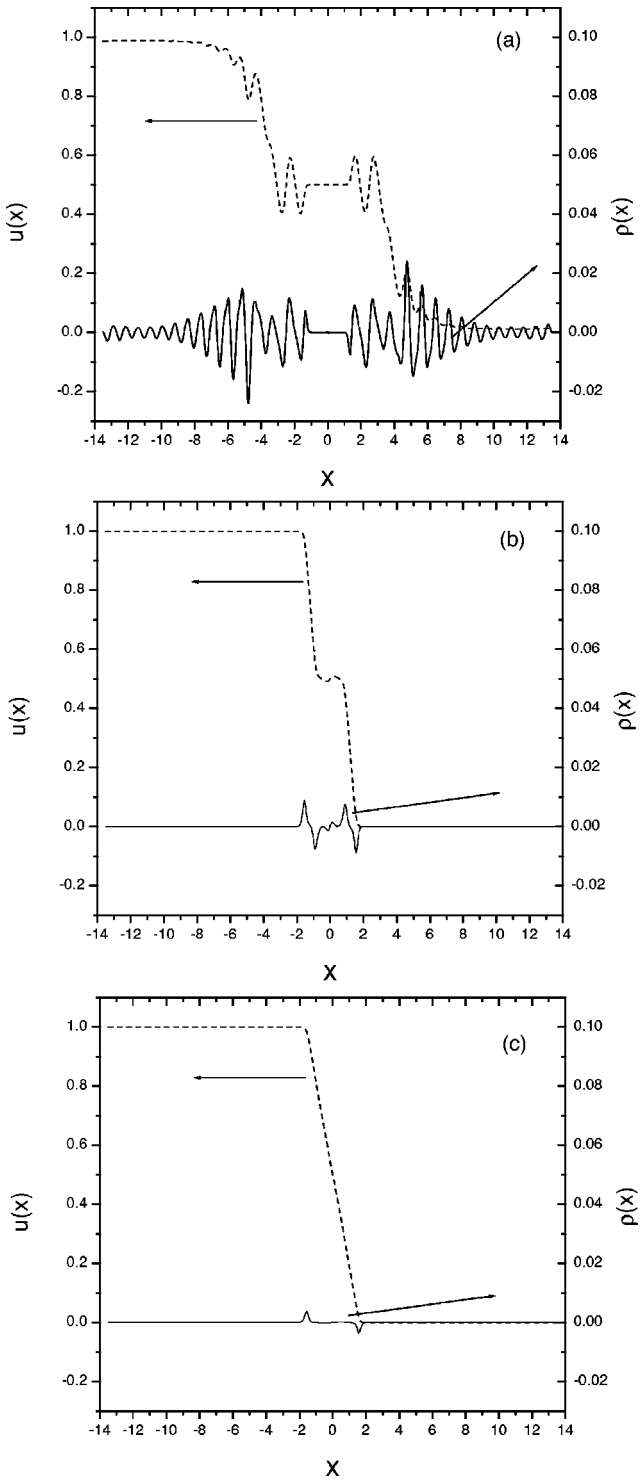

FIG. 2. Distributions of internal potential and charge density for (a) $\mu=1.805$, (b) $\mu=1.802$, and (c) $\mu=1.7$. Other parameters are $d=0.5$, $L_c=4$, $L_{co}=7.5$, $b=0.5$, $c=1$, and $W=20$. The energy is in unit of the transverse ground-state energy Δ of 1D leads, and length in unit of 1D portion width a ($=50$ nm).

coulomb interaction between the charges. In the presence of coulomb interaction, the more negatively charged layers induce positive charges in the neighboring less negatively charged layers. Hence, the intensive fluctuations in the charge density are expected. In the resonant case, the electrons can penetrate completely through the barrier, and the charges driven by the voltage neither stay around nor inside the conductor. And so, no potential drop is caused. In this case, the scattering of electrons is completely due to the nonuniform cross section in the transition regions, and this scattering results in the potential drops and charge accumulation in the transition regions. In our previous work[22] that was about a 1D double-barrier structure without contacts, the potential drop in the resonant case was almost zero [i.e. characteristic function $u(x)$ was constant : 1/2], and there is almost no charge accumulation throughout the system. We would like to remark that for the near resonance case (that is, large transmission probability but not equal to one), the distributions of internal potential as well as charge density are similar to that of the resonant case. In Fig. 2(b), we present the results for the case of small transmission probability ($\mu=1.802$). From the curve of $\rho(x)$, one finds that there is a considerable amount of charge distribution around the barrier regions as well as in the well region, but away from the double barrier in the leads and in the reservoirs there is no charge accumulation. In this case, the charges driven to the other side of the conductor penetrate through the double barrier with a small transmission probability. Thus, most of the charge carriers are reflected back into the 1D leads and reservoir. We then expect that there is no charge accumulation beyond the double barrier and hence the internal potential $u(x)$ should be constant ($=1$) beyond the double barrier (even in the transition regions), as shown in Fig. 2(b).The potential drop mainly happens within the double barrier, and the charges are distributed around and within the conductor. In Fig. 2(c), we show the result for the case where chemical potential ($\mu=1.7$) is far from the resonant energy ($E=1.805$) and for all channels the transmission probability is almost zero. The results in this case are qualitatively in agreement with that for the double-barrier system without contacts, where the characteristic function $u=1(0)$ on the left (right) side of the double-barrier conductor, and the curve of $u(x)$ is almost a straight line inside the conductor, and so the charge accumulation is nonzero only just beyond the two barriers. It is worth emphasizing that our results for the system with wide contacts show that the characteristic function tends to 1 (0) on the left (right) side the double-barrier conductor for both resonant and nonresonant cases. This fulfills the requirement of Büttiker's theory.[14]

IV. CAPACITANCE AND LOW-FREQUENCY ADMITTANCE

Having studied the distributions of internal potential and charge density that reveals certain information of the system under investigation, next we will study the capacitance and ac conductance, which may present a result that is capable of being directly verified with the experimental data. According to Eq. (12), when a small voltage δV is applied to the left reservoir ($\alpha=1$), the total charge accumulated in the left half portion of Ω is given by

$$\delta Q=\int_{x_L}^{x_{0L}}\delta q(x)dx,$$

and then the capacitance of the double-barrier system can be defined as

$$C=\frac{\delta Q}{\delta V}=\int_{x_L}^{x_{0L}}\rho(x)dx$$
$$=e^2\int_{x_L}^{x_{0L}}\left[\frac{dn_\alpha(x)}{dE}-\frac{dn(x)}{dE}u_\alpha(x)\right]dx, \tag{13}$$

where x_{0L} is the position of center of the left barrier. As in the well-known Coulomb blockde model for junction arrays, where one junction (barrier) corresponds to one capacitance, we regard the double-barrier system as two capacitors in series. It should be point out that it is difficult to give a precise definition of the capacitance for our system because our model is a continuous one, and generally the charge distribution shows an extensive fluctuation around zero. In the case of Figs. 2(a) and 2(c), the system can be regarded as a single capacitor, but in the case of Fig. 2(b) it would be invalid to regard it in this way.

With the information of partial density of states (PDOS), injectivities, and internal potentials, we can calculate the admittance for low frequencies[14–16]

$$g_{\alpha\beta}(\omega)=g_{\alpha\beta}(0)-i\omega e^2E_{\alpha\beta}, \tag{14}$$

where ω is the frequency of the ac bias, $g_{\alpha\beta}(0)$ is the dc conductance, and

$$E_{\alpha\beta}=e^2\frac{dN_{\alpha\beta}}{dE}-e^2\int dx\frac{dn_\alpha(x)}{dE}u_\beta(x) \tag{15}$$

is the emittance. In the first term of Eq. (15),

$$\frac{dN_{\alpha\beta}}{dE}=\frac{1}{4\pi i}\int dE\left(\frac{-\partial f}{\partial E}\right)\mathrm{Tr}\left[\mathbf{s}_{\alpha\beta}^\dagger\frac{d\mathbf{s}_{\alpha\beta}}{dE}-\frac{d\mathbf{s}_{\alpha\beta}^\dagger}{dE}\mathbf{s}_{\alpha\beta}\right] \tag{16}$$

are the partial densities of states, and may be interpreted as the carrier density of states in volume Ω, corresponding to those carriers injected from reservoir β and going out of reservoir α. It should be noticed that Eq. (16) is exact only when Ω is infinite ($|x_L|\rightharpoonup\infty$).[23] For the finite-size system, PDOS can be defined as[14,15]

$$\frac{dN_{\alpha\beta}}{dE}=\frac{-1}{4\pi i}\int dE\left(\frac{-\partial f}{\partial E}\right)\mathrm{Tr}\left[\mathbf{s}_{\alpha\beta}^\dagger\frac{d\mathbf{s}_{\alpha\beta}}{dU}-\frac{d\mathbf{s}_{\alpha\beta}^\dagger}{dU}\mathbf{s}_{\alpha\beta}\right], \tag{17}$$

where

$$\frac{d\mathbf{s}_{\alpha\beta}}{dU}=\int_{x_L}^{x_R}\frac{\delta\mathbf{s}_{\alpha\beta}}{\delta U(x)}dx. \tag{18}$$

$d\mathbf{s}_{\alpha\beta}/dU$ can be calculated as the following. In the considered region Ω, introducing a constant potential U, we repeat the above process of calculating the wave functions, and get the scattering matrix $\mathbf{s}_{\alpha\beta}(E,U)$. Alternatively, we can set the electron ''energy'' as E' and E in and out of the region Ω, respectively, and get $\mathbf{s}_{\alpha\beta}(E,E')$. We then have

$$\frac{d\mathbf{s}_{\alpha\beta}}{dU}=\int_{x_L}^{x_R}\frac{\delta\mathbf{s}_{\alpha\beta}}{\delta U(x)}dx=\left.\frac{d\mathbf{s}_{\alpha\beta}(E,U)}{dU}\right|_{U=0}$$
$$=-\left.\frac{d\mathbf{s}_{\alpha\beta}(E,E')}{dE'}\right|_{E'=E}. \tag{19}$$

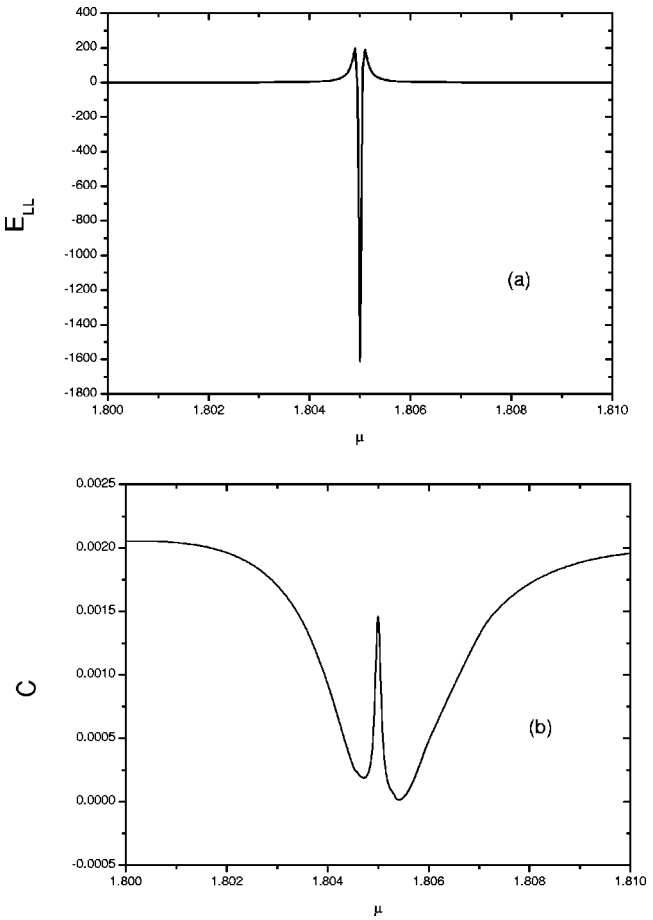

FIG. 3. The plots of emittance (a) and capacitance (b) as functions of chemical potential μ, around the resonant energy. The other parameters are the same as in Fig. 2. The energy and length units are taken as above.

In Figs. 3(a) and 3(b), we present the capacitance C and diagonal emittance E_{11}, respectively, as functions of chemical potential around the resonant energy. The diagonal emittance is always positive (showing a capacitive behavior) when chemical potential μ is not too close to the resonant energy, but when the chemical potential is close to (or exactly equal to) the resonant energy, the emittance is negative and gives a very great negative peak (showing an inductive behavior). This is qualitatively in agreement with the discrete model results obtained by Prêtre *et al.*[17] and with our previous results (continuous model)[22] for the case without contacts. Figure 3(b) shows the capacitance around the reso-

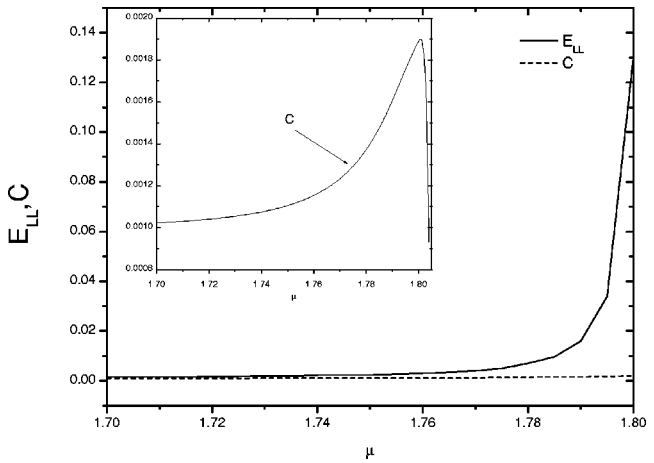

FIG. 4. The plots of emittance and capacitance as functions of chemical potential μ, which start from far away from the resonant energy. The other parameters are the same as in Fig. 2, and the energy and length units are taken as above. Inset: the plot of capacitance that displays a peak at above $\mu=1.80$.

nance. From this figure, we find that when the chemical potential approaches to the resonant energy, the capacitance decreases first, and then increases sharply making a sharp peak at the resonant energy. This is very different from the case without contacts where the charge accumulation is vanishingly small at the resonance. Moreover, our results show that the amplitude of the emittance around the resonant energy is much greater than the capacitance, and at the resonance the capacitance has a peak while the emittance makes a great negative peak.

We believe that this peak originates from the contact effect, and a plausible explanation can be presented as follows. When the Fermi level is right at the resonant energy, the behavior of this system is similar to the case of a quantum wire (QW) with contacts, and with one channel open. According to the previous work,[25] with the increasing Fermi level, a quasiplateau of capacitance would appear after one channel is open. Here, in our case, the resonant energy 1.805 is at the front part of the plateau, so the capacitance should be quite large. On the other hand, when the Fermi level moves away a little bit from the resonant energy, the potential drop around the barriers will rapidly increase because the resonant width is very narrow. Meanwhile, the potential variation in the transition region is greatly reduced and becomes very small, hence the charge accumulation in the region vanishes rapidly, resulting in a drop of capacitance and therefore, the formation of such a peak. We conclude that the behavior of capacitance is very different as compared to the case without contacts: a sharp peak occurs at the resonant energy. However, the feature of negative peak of E_{11} (in the case without contacts) is unchanged in the presence of contacts.

In Fig. 4, we present the capacitance $C(\mu)$ and emittance $E_{11}(\mu)$, starting with the chemical potential far away from the resonant energy. One can find that the emittance and capacitance tend to same values when the chemical potential is far away from the resonant energy, this is expected, but when the system approaches to the resonance both the emittance and capacitance increase. The increase of emittance is much more rapid, and the difference of them is enlarged rapidly. Moreover, the capacitance reachs a peak (which is wider as compared to the resonant peak) when the chemical potential is about 1.8, and there is another wide peak in the capacitance at symmetrical position to $\mu=1.8$ about the sharp resonant peak. We would like to point out that in the case without contacts, two similar peaks of the capacitance occur at the same positions as the positive (capacitive) peaks of the emittance. It is clear from Fig. 4 that the presence of contacts changes the location of these two peaks of the capacitance.

V. CONCLUSION

In conclusion, by employing the scattering theory developed by Büttiker *et al.*, we have studied the dynamical response of the double-barrier system, in which the 1D double barrier and two 2D reservoirs are included. We have presented the calculation of various physical quantities such as the distributions of internal potential and charge density, capacitance, and low-frequency ac conductance. The results of the internal potential and the charge density show that the induced charge density has an antisymmetric distribution profile about the well center, and the characteristic potentials would tend to unity (zero) deep in the reservoirs. When the system is far away from resonance, although some quantum channels are open, the transmission probability is very small. In this case, the antisymmetric charge distribution exists only around the barrier regions as a response to the applied voltage, and hence the contacts almost have no effect on the results. For the case of small transmission probability, we found a considerable amount of charge accumulation around the conductor, but there is almost no potential drop outside it. As for the cases of resonance or near resonance (with a large transmission probability for an open channel), there is no charge accumulation inside the double-barrier conductor. However, there are intensive fluctuations of the charge density in the transition regions between the contacts (2D) and the double barrier (1D). In this case, the effect of contacts on the charge and potential distributions is considerable. It is found from the calculation of ac conductance that qualitatively the presence of contacts does not change the main features of the emittance without contacts, i.e., the negative peak (inductive behavior) and the positive peaks (capacitive behavior). However, the effect of contacts on the capacitance is significant when the chemical potential is very close to the resonant energy: causing a capacitance peak at the resonance. This peak is clearly due to the charge accumulation in the transition regions between the 1D and 2D portions.

ACKNOWLEDGMENTS

The work was partially supported by the postdoctoral program (G-YW68) of The Hong Kong Polytechnic University.

[1] J. Voit, Rep. Prog. Phys. **58**, 977 (1995).
[2] H.J. Schulz, G. Cuniberti, and P. Pieri, cond-mat/9807366 (unpublished).
[3] D.L. Maslov and M. Stone, Phys. Rev. B **52**, R5539 (1995).
[4] V.V. Ponomarenko, Phys. Rev. B **52**, R8666 (1995).
[5] I. Safi and H.J. Schulz, Phys. Rev. B **52**, R17 040 (1995).
[6] A. Yacoby, H.L. Stormer, N.S. Wingreen, L.N. Pfeiffer, K.W. Baldwin, and K.W. West, Phys. Rev. Lett. **77**, 4612 (1996).
[7] A.Yu. Alekseev and V.V. Cheianov, Phys. Rev. B **57**, R6834 (1998).
[8] V.A. Sablikov, S.V. Polyakov, and M. Büttiker, Phys. Rev. B **61**, 13 763 (2000).
[9] F.D.M. Haldane, J. Phys. C **14**, 2585 (1981).
[10] M. Büttiker, H. Thomas, and A. Pretre, Phys. Lett. A **180**, 364 (1993).
[11] T. Christen and M. Büttiker, Phys. Rev. Lett. **77**, 143 (1996).
[12] P.W. Brouwer and M. Büttiker, Europhys. Lett. **37**, 441 (1997).
[13] J. Wang and H. Guo, Phys. Rev. B **54**, R11 090 (1996).
[14] M. Büttiker, J. Phys.: Condens. Matter **5**, 9361 (1993).
[15] M. Büttiker, H. Thomas, and A. Pretre, Z. Phys. B: Condens. Matter **94**, 133 (1994).
[16] M. Büttiker, A. Pretre, and H. Thomas, Phys. Rev. Lett. **70**, 4114 (1993).
[17] A. Pretre, H. Thomas, and M. Büttiker, Phys. Rev. B **54**, 8130 (1996).
[18] Ya.M. Blanter and M. Büttiker, Europhys. Lett. **42**, 535 (1998).
[19] V.A. Sablikov and B.S. Shchamkhalova, Phys. Rev. B **58**, 13 847 (1998).
[20] Büttiker and Christen, in ''*Mesoscopic Electron Transport*,'' edited by Lydia L. Sohn, Leo P. Kouwenhoven, and Gerd Schon (Kluwer Academic, Dordrecht, 1997), pp. 259–289.
[21] X. Zhao and Y.X. Chen, Phys. Rev. B **64**, 085326 (2001).
[22] W.Z. Shangguan, T.C. Au Yeung, Y.B. Yu, C.H. Kam, and X. Zhao, Phys. Rev. B **65**, 235315 (2002).
[23] Q. Zheng, J. Wang, and H. Guo, Phys. Rev. B **56**, 12 462 (1997).
[24] M. Büttiker and T. Christen, in ''*Quantum Transport in Semiconductor Submicron Structures*,'' edited by B. Kramer (Kluwer Academic Publisher, Netherlands, 1996), pp. 363–291.
[25] Y.B. Yu, T.C. Au Yeung, and W.Z. Shangguan, Phys. Rev. B **66**, 235315 (2002).